

# Influence of lead Doping on structural and optical properties of thermal evaporation Thin Films of

## $Pb_xSe_{1-x}$

Izzat M.Al-Essa\*, Mahdi H.Suhail\* and Ahmed Jumma Noori\*\*

\*Dept. of Physics, College of Science, University of Baghdad, Jadiriya, Baghdad, Iraq

\*\*Directorate of Education Salahuddin, Education department of Tuz, Karkuk, Iraq

E-mail: mhsuhail@yahoo.com

**Abstract:**  $Pb_xSe_{1-x}$  alloys for different lead ( $X=0.1, 0.2, 0.3,$  and  $0.4$ ) was prepared inside quartz vacuum tube. The tube was sealed and heated to melting point (950 K) and left for five hours to get homogenous compound and then allowed to cool slowly to room temperature. X-ray diffraction spectrum appeared that all alloys and films have polycrystalline structure with hexagonal Wurtzite phase at ( $X=0.1$ ) and a mixture phase of hexagonal and cubic at ( $X=0.2, 0.3, 0.4$ ). The preferred orientation was (111). The surface morphology of the thermally prepared  $Pb_xSe_{1-x}$  thin films was investigated by means of atomic force microscopy (AFM). The optical characteristics of the films prepared on quartz substrates measurement showed that  $Pb_xSe_{1-x}$  films have direct energy gap ( $E_g$ ) which decreases with increasing Pb content. Also the optical constant such as refractive index, extinction coefficient and dielectric constant has been calculated. In the present work, we study the effect of different concentration on the structural and optical properties of  $Pb_xSe_{1-x}$  thin films which prepared by thermal evaporation.

### 1-INTRODUCTION

Metal chalcogenide compounds, which are semiconductor in nature, are of considerable technical interest in the field of electronics and

electro-optical devices [1] Lead selenide (PbSe) is an important semiconducting material and has been extensively investigated for infrared detectors, photographic plates, photodetectors, photoresistors, photoemitters in the infrared (IR) and also in solar cell technology [2-5]. PbSe is a narrow direct band gap semiconductor material [6,7] with useful electrical, optical and lattice properties [8,9]. The large Bohr exciton radius (of about 46nm) and multiple exciton generation in PbSe makes it a suitable system to study quantum confinement effects on electrons and holes [10-12] and with higher optical efficiency has renewed interest in the optical properties of PbSe [7]. low thermal conductivity of PbSe also makes it a suitable thermoelectric material [13, 14]. PbSe has the cubic NaCl-type structure [15].

The full width at half maximum (FWHM) of the peak is a measure of the grain size as described by Scherers formula[16]:

$$G.S = \frac{0.89\lambda}{\Delta(2\theta) \cdot \cos\theta} \dots\dots\dots(1)$$

where  $\theta$  is the Bragg angle and  $\lambda$  is the wavelength of the source of radiation [Cu( $k_\alpha$ ) with  $\lambda=1.5406\text{\AA}$ ].

Above the exponential tail, the absorption coefficient ( $\alpha$ ) has been reported to obey the following equation [17],  $\alpha(\nu)h\nu = B(h\nu - E_g)^r \dots\dots\dots(2)$

Where  $\nu$  is the frequency of the incident beam, B is a constant,  $E_g$  is the optical band gap and  $n$  is an exponent, which can be assumed to have values depending on the nature of the electronic transition [18,19].

The absorption coefficient in this region can be described by Urbach formula[20,21]:

$$\alpha = \alpha_o \cdot \exp\left(\frac{\Delta E}{h\nu}\right) \dots\dots\dots(3)$$

$h\nu$ : is the photon energy and  $\Delta E$ : is the width of localized levels into energy gap.

The extinction coefficient ( $k$ ) characterizes absorption of the electromagnetic wave energy in the process of propagation of a wave through a material and equal to:

$$k = \frac{\alpha\lambda}{4\pi} \dots\dots\dots(4)$$

The normal-incidence reflectivity  $R$  can also be given by [22]:

$$R = \frac{(n-1)^2 + K^2}{(n+1)^2 + K^2} \dots\dots\dots(5)$$

Then the refraction index value can be calculated from the formula [23]:

$$n = \sqrt{\frac{4R}{(R-1)^2} - k^2} - \left[\frac{(R+1)}{(R-1)}\right] \dots\dots\dots(6)$$

The complex index of refraction ( $n_c$ ) is defined as [24]:

$$n_c = n + ik = \epsilon^{1/2} = [\epsilon_1 + i\epsilon_2]^{1/2} \dots\dots\dots(7)$$

The optical constants,  $n$  and  $k$ , are real and positive numbers, and can be determined from optical measurements. From Equation (7), it follows that[25]

$$\epsilon_1 = n^2 - k^2 \dots\dots\dots(8)$$

$$\epsilon_2 = 2nk \dots\dots\dots(9)$$

## 2- Experimental work

The  $Pb_xSe_{1-x}$  alloy with ( $X=0.1, 0.2, 0.3, 0.4$ ) have been successfully prepared using high purity (99,999%) of lead and selenium metal obtained from Balzer's company. Each element weighted according to its atomic weight and then mixing in quartz tube (length=25 cm, diameter =0.9 cm) evacuated at pressure of  $10^{-3}$  mbar. The tube was sealed and heated in electrical program controller furnace of type (Qallenhamp) at temperature 950 K for about 5 hours and then allowed to cool slowly to room temperature. After that the ampoule was broken and the prepared compound was taken out and examined by X-ray diffraction to be sure of the purity and structure of the compound. The powder of the compounds was used as a source of the of the evaporation to prepare the films. The glass and quartz substrates are freshly cleaned with a pure alcohol and distilled water followed by ultrasonic agitation. Thin films of different concentration are prepared onto glass and quartz substrates at room temperature using Edward coating unit (model E306A) of vacuum  $10^{-5}$  torr. A molybdenum boat is used as the evaporation source and the substrates are placed directly above the source at a distance of nearly 15cm. The structure of these films grown on glass substrates was examined by a (phillips PW) X-ray diffractometer with  $CuK_{\alpha}$  radiation of the wavelength ( $\lambda=1.541 \text{ \AA}$ ) and radiation target in the range of  $2\theta$  between  $20-60^\circ$ . The surface morphology of the films is investigated by atomic force microscopy (SPM, Model-AA3000). The transmission and absorption spectra is recorded using FTIR spectrophotometer (Model- Lambda FTIR-7600) in the range 2500-4250nm, at room temperature. The optical properties was calculated as a function wavelength in the range 350-1100nm.

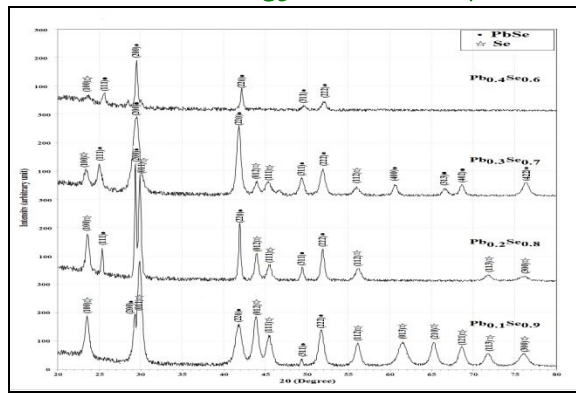
## 3-Results and discussion

### 3-1 X-ray diffraction of $Pb_xSe_{1-x}$ alloys and thin films

The X-ray diffraction patterns for ( $Pb_xSe_{1-x}$ ) powders at different concentration ( $X=0.1, 0.2, 0.3$ , and  $0.4$ ), are shown in figure (1).

The observation of the X-ray peaks for all  $Pb_xSe_{1-x}$  powders indicates that the structure of these alloys are polycrystalline with cubic and hexagonal phase.

The grain size is calculated by using equation (1). The grain size for (200) plane is (39.3Å, 39.3Å, 9.1Å, 28.6 Å) for powder at ( $X=0.1,0.2,0.3$ ,and  $0.4$ )respectively and agreement with the standard values for the hexagonal and cubic structure.



Fig(1) X-ray diffraction patterns for  $Pb_xSe_{1-x}$  powder with different Pb content ( $x= 0.1, 0.2, 0.3$  &  $0.4$ )

The observed d-values with standard (JCPDS-ICDD file NO, 96-901-1360 and 96-901-2502 ) for  $Pb_xSe_{1-x}$  powder. The results compared with ASTM card are in a good agreement .

The crystal structure of  $Pb_xSe_{1-x}$  films, which were evaporated on glass substrates with thickness ( $150\pm 20$ ) nm at room temperature are shown in figure (2) . The films are polycrystalline with hexagonal structure at ( $X=0.1$ ) . The structure become a mixture of cubic and hexagonal at ( $X=0.2,0.3$  and  $0.4$ ). The preferred orientation lies along (200) direction . Our results are nearly in agreement with Al-Woaeli[26] and Kassim etal [ 27].

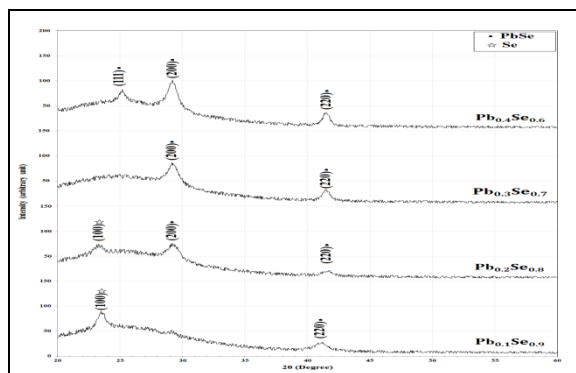


Fig. (2) X-ray diffraction patterns of ( $Pb_xSe_{1-x}$ ) thin films prepared at room temperature with different  $x$  ( $0.1, 0.2, 0.3$  and  $0.4$  ).

The results compared with ASTM card were in a good agreement as shown in table(2). The grain size for (220) plane is (6.8Å, 9.1Å, and 10.8 Å) for powder at ( $X= 0.2,0.3$ ,and  $0.4$ )respectively.

Table (2) Structural Parameters ,Inter-planar Spacing, Crystalline Size of ( $Pb_xSe_{1-x}$ ) thin films prepared at room temperature with different  $x$  ( $0.1, 0.2, 0.3$  and  $0.4$  ).

X	2θ (Deg.)	FWHM (Deg.)	d <sub>hkl</sub> Exp. (Å)	hkl	phase	d <sub>hkl</sub> Std. (Å)	G.S (nm)
0.1	23.534	0.738	3.777	(100)	Se	3.7812	11.0
	41.087	1.243	2.195	(220)	PbSe	2.1586	6.8
0.2	23.301	0.738	3.814	(100)	Se	3.7812	11.0
	29.282	1.126	3.048	(200)	PbSe	3.0527	7.3
	41.553	0.932	2.172	(220)	PbSe	2.1586	9.1
0.3	29.243	1.087	3.052	(200)	PbSe	3.0527	7.6
	41.584	0.842	2.170	(220)	PbSe	2.1586	10.1
0.4	25.204	0.583	3.531	(111)	PbSe	3.5250	14.0
	29.204	0.971	3.056	(200)	PbSe	3.0527	8.5
	41.962	0.789	2.151	(220)	PbSe	2.1586	10.8

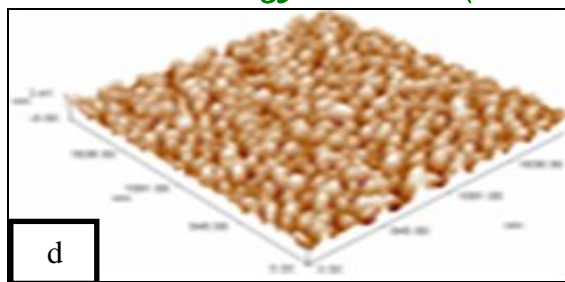


Fig. (3-a, b, c and d) AFM image for (Pb<sub>x</sub>Se<sub>1-x</sub>) with different x (0.1, 0.2, 0.3 and 0.4) respectively

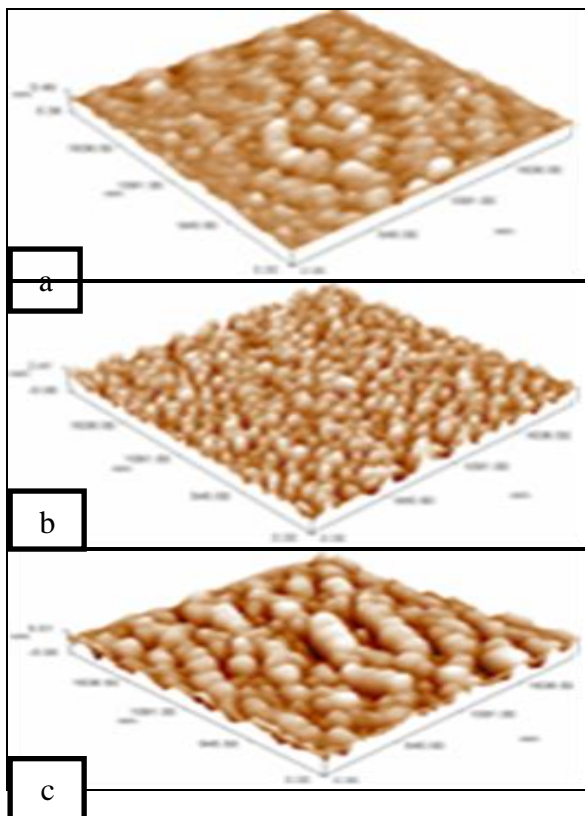
Table (3) show the value of average roughness, average grain size (grain diameter) and root mean square roughness (RMS). It is observed from this table that the average roughness value decreasing with increase the lead content. This is may be due to the rearrangement of atom in film and reduce the vacancy defect. On the other hand from the same table the we can see the value of RMS and G.S decrease and increases but in nonsystematic sequence with the increase of lead content. This behavior can be explained on the basis that addition of Pb to Pb<sub>x</sub>Se<sub>1-x</sub> binary system reduces the local structure since it leads to some degree of disordering.

Table (3) The Value of Average Roughness, RMS and average grain size for Pb<sub>x</sub>Se<sub>1-x</sub> with different x (0.1,0.2,0.3 and 0.4)

P <sub>x</sub> Se <sub>1-x</sub>	Average Roughness (nm)	RMS(nm)	Average grain size (nm)
0.1	0.393	0.504	83.49
0.2	0.375	0.455	71.29
0.3	0.377	0.473	76.06
0.4	0.937	1.14	97.26

**3-2 Morphology properties of (Pb<sub>x</sub>Se<sub>1-x</sub>) thin film**

The morphological characteristics of Pb<sub>x</sub>Se<sub>1-x</sub> thin films have been deposited on glass substrates at room temperature have been studied using Atomic Force Microscope (AFM). Figure (3) shows the surface topographical images recorded for Pb<sub>x</sub>Se<sub>1-x</sub> thin films grown by thermal evaporation.



**3-3 Optical properties of Pb<sub>x</sub>Se<sub>1-x</sub> thin films :**

Figure (4) show the variation of absorbance as a function of wavelength for different Pb content. The absorbance increase with increasing of Pb content. The increases in the absorbance means increase in the reflection occurs due to the increase of Pb content in the composition, where Pb metal increases the reflection. The increase could be attributed to the increasing in the degree of the crystallinity of film structure by increasing the grain size.

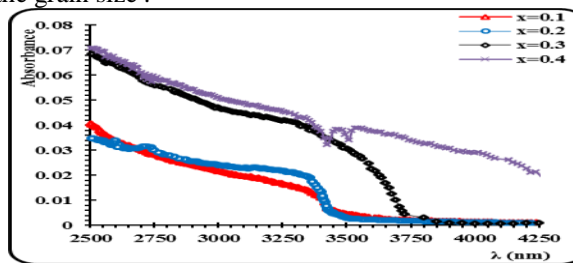


Fig.(4) Absorbance vs. the wavelength for Pb<sub>x</sub>Se<sub>1-x</sub>

Figure (5) which shows the variation of absorption coefficient as a function of wavelength for  $Pb_xSe_{1-x}$  films. The absorption coefficient decreases with increasing wavelength transition and have the same behavior of the absorbance since they were calculated according to equation (4). This behavior may be due to reduce the recombination process and improvement in the crystallinity of films then reduce the density of localized states [28] which coincides with the XRD results. The value of absorption coefficient for  $Pb_xSe_{1-x}$  at (2750nm) wavelength is tabulated in Table (4).

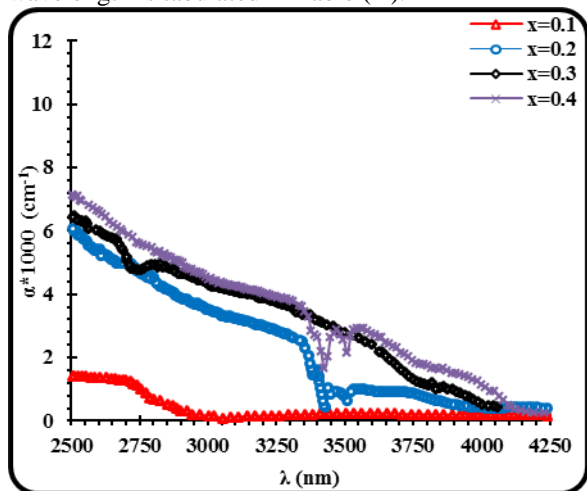


Fig.(5) The absorption coefficient vs. the wavelength for ( $Pb_xSe_{1-x}$ ) at (0.1,0.2,0.3and0.4)

The optical energy gap ( $E_{gop}$ ) was derived assuming a direct transition between the edge of the valence and conduction band. The optical energy gap values ( $E_{gop}$ ) for  $Pb_xSe_{1-x}$  films have been determined by using Tauc formula equation (2) by plotting the relations of  $(ahv)^2$  vs  $E$  (eV) for direct energy gap as shown in figure(6) at different value of  $x$ . We can observe that the increasing in lead content go to decreases the energy gap from  $E_{gop} = 0.44$  eV to  $E_{gop} = 0.40$  eV when increase the lead content from 0.1 to 0.4. The decreases in the energy gap means increase in the reflection occurs due to the increase of lead content(metal increases the reflection) in the composition.

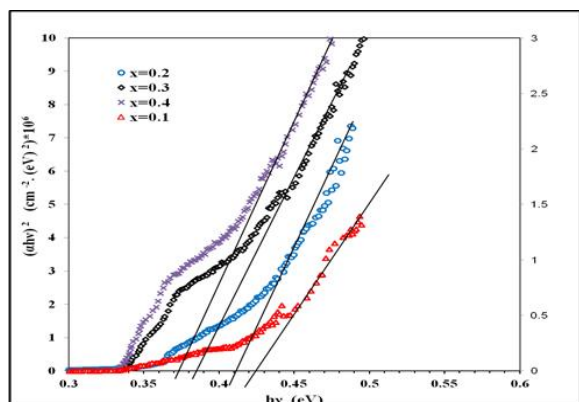


Fig.(6)  $(ahv)^2$  versus photon energy( $hv$ )for( $Pb_xSe_{1-x}$ ) at different ( $X=0.1,0.2,0.3$ and $0.4$ ).

The refractive index ( $n$ ) calculated using equation(6). Figure (7) show the variation of refractive index with wavelength for  $Pb_xSe_{1-x}$  films at different value of  $x$  ( $X=0.1,0.2,0.3$ and $0.4$ ). It is clear that the refractive index decreases with increasing the wavelength. Table (4) show the values of refractive index ( $n$ ) for all films with different value of  $x$ . This increase with increasing of  $X$  is attributed to the increase in packing density and the decrease in degree of amorphosity.

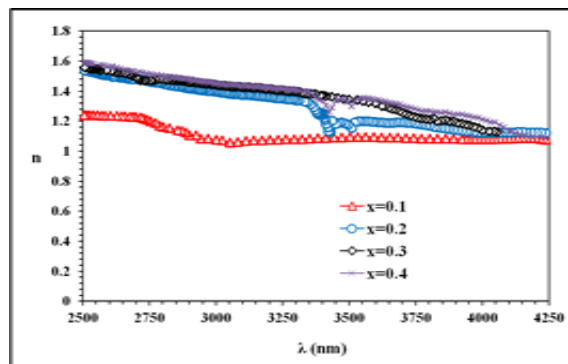


Fig.(7) The refractive index vs. the wavelength for  $Pb_xSe_{1-x}$  at ( $X=0.1,0.2,0.3$ and $0.4$ ).

The extinction coefficient ( $k$ ) is determined by using equation (4).The relation between the extinction coefficient and wavelength for  $Pb_xSe_{1-x}$  films deposited at values of  $x$  is shown in Figure(7). From this figure it is found that the extinction coefficient ( $k$ ) takes the similar behavior of the corresponding absorption coefficient. One can deduce from this figure that the extinction coefficient decreased with increasing the wavelength.

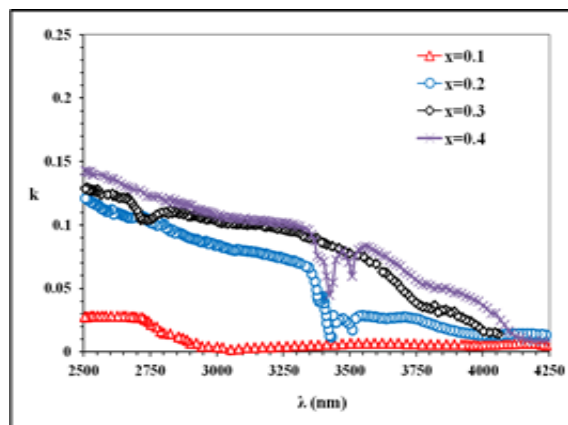


Fig.(8) The extinction coefficient vs. the wavelength for( $Pb_xSe_{1-x}$ ) at ( $X=0.1,0.2,0.3$ and $0.4$ ).

The dielectric constant ( $\epsilon$ ) consists of real part ( $\epsilon_r$ ) and imaginary part ( $\epsilon_i$ ) as a function of wavelength for  $Pb_xSe_{1-x}$  films are shown in figures 9 and 10 respectively.

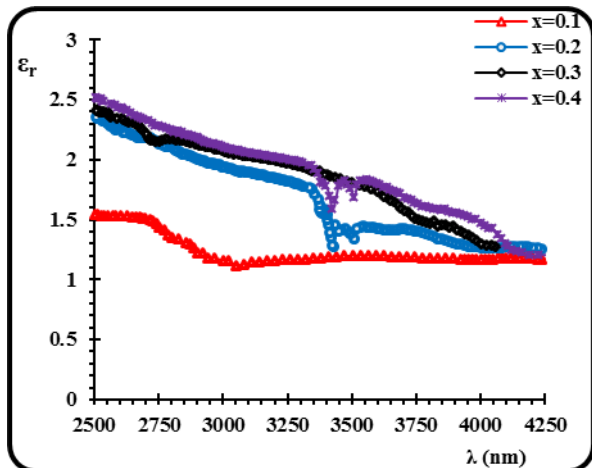


Fig.(9) The real part of dielectric constant vs. the wavelength for ( $Pb_xSe_{1-x}$ ) at ( $X=0.1, 0.2, 0.3$  and  $0.4$ ).

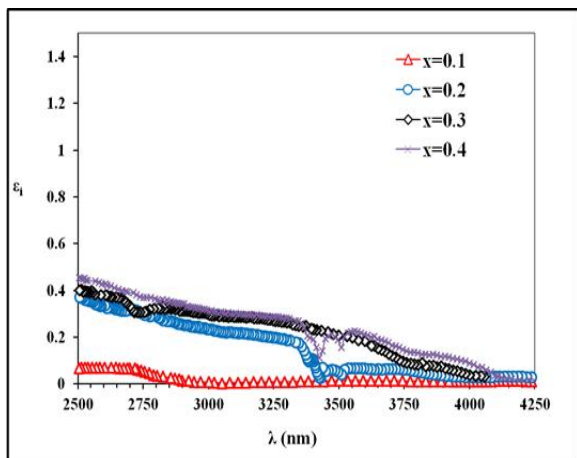


Fig.(10) The imaginary part of dielectric constant vs. the wavelength for  $Pb_xSe_{1-x}$  at  $x$  ( $0.1, 0.2, 0.3$  and  $0.4$ ).

The value of Dielectric Constants ( $\epsilon_r$  and  $\epsilon_i$ ) since they were calculated according to equation (8) and equation (9).

The variation of  $\epsilon_r$  and  $\epsilon_i$  with the increase of the wavelength of the incident radiation is due to the change of reflectance and absorbance [29]. The behavior of  $\epsilon_r$  is similar to that of the refractive index because of the smaller value of  $k^2$  compared with  $n^2$ , while  $\epsilon_i$  mainly depends on the  $k$  value, which are related to the variation of absorption coefficient. Real ( $\epsilon_r$ ) and imaginary ( $\epsilon_i$ ) parts for  $Pb_xSe_{1-x}$  is tabulated in Table (4) at (2750nm) wavelength.

Table (4) The optical parameters of  $Pb_xSe_{1-x}$  with different ( $X=0.1, 0.2, 0.3$  and  $0.4$ ) at wavelength 2750nm

Pb concentration	Abs.	$\alpha$ $cm^{-1}$	$k$	$n$	$\epsilon_r$	$\epsilon_i$
0.1	0.007	1004	0.02	1.20	1.44	0.05
0.2	0.006	888	0.03	1.19	1.41	0.06
0.3	0.031	4786	0.10	1.47	2.15	0.31
0.4	0.036	5596	0.12	1.51	2.28	0.37

#### 4- Conclusion:

$Pb_xSe_{1-x}$  alloys for different lead ( $X=0.1, 0.2, 0.3$ , and  $0.4$ ) have been successfully prepared inside quartz vacuum tube. The x-ray analysis showed that the  $Pb_xSe_{1-x}$  alloys and films at different Pb content are polycrystalline with a hexagonal of wurtzite type for a compound at ( $X=0.1$ ) and mixture of hexagonal and cubic for other compound at ( $X=0.2, 0.3, 0.4$ ). The morphological characteristics of ( $Pb_xSe_{1-x}$ ) thin films have been studied and show the average roughness and average grain size values increasing with increase the (Pb) content for all samples. From the FTIR absorbance spectra, we found that the absorbance increase with increasing of Pb content. Energy gap decrease with increase of Pb content while the refractive index, extinction coefficient and the variation of the real and imaginary parts of the dielectric constant decreases with increasing the wavelength, and all parameter above was found to increasing when the Pb concentration increasing.

#### References:

- [1] A. Merouani and H. A. Ammardjia, Study of Properties of Lead Selenide ( $PbSe$ ) Thin Films Deposited on  $TiO_2$ , *Journal of Energy and Power Engineering*, Vol.7 pp. 2100-2105, 2013.
- [2] Grozdanov, I., M. Najdoski, and S.K. Dey. *Materials Letters*, Vol. 38, pp. 28-32, 1999.
- [3] Gautier, C., G. Breton, M. Nouaoura, M. Cambon, S. Charar, and M. Averous. *Thin Solid Films*, Vol.315, pp.118-122, 1998
- [4] Avellaneda, D., M.T.S. Nair, and P.K. Nair. *Thin Solid Films*, Vol. 517, pp.2500-2502, 2009.
- [5] Ezenwa I. A., Optical Properties of Chemical Bath Deposited Lead Selenide Thin Films, *Advances in Applied Science Research*, Vol. 3, No.2, pp.980-985, 2012.
- [6] O. Madelung, U. Ressler, and M. Schulz, Springer Materials - The Landolt-Brnstein Database, 2010.

- [7] C. S. Lent, M. A. Bowen, J. D. Dow, R. S. Allgaier, O. F. Sankey, and E. S. Ho, Superlattices and Microstructures, Vol.2, 491,1986.
- [8] J. Diezhandino, G. Vergara, G. Pérez, I. Genova, M. T. Rodrigo, F. J. Sánchez, M. C. Torquemada, V. Villamayor, J. Plaza, I. Catalán, R. Almazán, M. Verdú, P. Rodríguez, L. J. Gómez, and M. T. Montojo, Applied Physics Letters, Vol.83, 2751,2003.
- [9] M. Ji, S. Park, S. T. Connor, T. Mokari, Y. Cui, and K. J. Gaffney, Nano Letters, Vol. 9, 1217,2009.
- [10] W. Liang, A. Hochbom, M. Fardy, M. Zhang, and P. Yang, Nano Research, Vol. 2, 394,2009.
- [11] K. S. Cho, D. V. Talapin, W. Gaschler, and C. B. Murray, Journal of American Chemical Society, Vol.127, 7140,2005.
- [12] Y. Gai, H. Peng, and J. Li, Jour. Phys. Chem. C, Vol.113, 21506,2009.
- [13] I. Kudman, Jour. of Mat. Science, Vol. 7, 1027,1972.
- [14] I. Kang and F. W. Wise, J. Opt. Soc. Am. B, Vol. 14, 1632,1997.
- [15] Hiroi Z, Nakayama N, Bando Y. J Appl Phys, Vol. 61,206,1987.
- [16] Springholz G., Holy V., Abtin L, Shape and composition of buried PbSe quantum dots determined by scanning tunneling microscopy, Appl. Phys. Lett., Volume 90, 2007.
- [17] Tauc J. In: Tauc J, editor. Amorphous and liquid semiconductors. New York: Plenum press; 1979.
- [18] Smith RA. Phil Mag Suppl; Vol.2,81,1953.
- [19] Caudhari S, Biswas SK, Chaudhary A. J Non-Cryst Solids, Vol.23,4470,1998.
- [20]F. Urbach, Phys. Rev. Vol. 92 pp 1324-1325,1953.
- [21] C. F. Klingshirm, “**Semiconductor Optics**”, Springer-Verlag Berlin Heidelberg, Now York, 1995.
- [22]Sadao Adachi, Properties of Group-IV, III–V and II–VI Semiconductors, John 55Wiley & Sons Ltd, The Atrium, Southern Gate, Chichester, West Sussex PO19 8SQ, England, Copyright © 2005, P 213
- [23]Chin-Lin Chen, Elements of optoelectronics and Fiber optics, School of Electrical and Computer Engineering, Purdue university, 1996.
- [24]A .Beiser, Concept of Modern Physics, Second Edition, Mc Graw –Hill, Kogakusha, LED.1973.
- [25]K.J.Kramer, S.Talwar,E.Ishiba, K.H.Weiner and T.W.Sigmon, Appl.Surf. Scien, Vol.69, No.2, pp. 121-126,1993.
- [26] Morooj Ali Al-Woaely, fabrication and study physical properties of PbSe detector),M.Sc. Thesis, University of Baghdad,2005 .
- [27]A. Kassim, S.M. Ho, A.H. Abdullah and S. Nag lingam, XRD, AFM and UV-Vis Optical Studies of PbSe Thin Films Produced by Chemical Bath Deposition Method, Chemistry & Chemical Engineering, Sharif University of Technology, Vol. 17, No. 2, pp. 139{143, 2010.
- [28] D. Albin, D. Rose, R. Dhere, D. Levi, L. Woods, Swartzlander-Guest, and P. Sheldon, Comparison of Close-Spaced Sublimated and Chemical Bath Deposited CdS Films: Effects on CdTe Solar Cells, Proc. 26th IEEE Photovoltaic Specialists Conf., p. 367,1997.
- [29]G.I. Rusu, P. Prepelita and N. Apetraoei, “Journal of Optoelectronics and Advanced Materials”, Vol.7, No.2, P. 829, 2005 .